The large change in hf for atoms with different environments (ΔH) is interpreted as due to *local* deviations in the conduction electron and core effects as described empirically by Bernas and Campbell.[8]

Assuming that the magnetic moment on the Mo atom is composition-independent, one obtains

$$\frac{1}{\mu^{\circ}_{\mathrm{Fe}}}\frac{d\bar{\mu}}{dC}+1=\frac{1}{\mu^{\circ}_{\mathrm{Fe}}}\frac{d\mu_{\mathrm{Fe}}}{dC}+\frac{\mu_{\mathrm{Mo}}}{\mu^{\circ}_{\mathrm{Fe}}}, \quad (3)$$

where $d\bar{\mu}/dC$ is the change in average moment per atom as seen by saturation magnetization, and $\mu^{\circ}_{\mathrm{Fe}}$ is the magnetic moment of pure iron. Using Eq. (2), and combining the value of $k=0.25\pm0.07$ for the composition of most uniform iron moment distribution, 6 at. % Mo, with the value of $d\bar{\mu}/dC=-2.10\pm0.04$ determined for *Fe*Mo in the recent saturation magnetization measurements of Aldred,[12] one obtains $\mu_{\mathrm{Mo}}=-0.4\pm0.2\mu_B$ for the magnetic moment on the Mo impurity site, where the negative sign indicates a moment oppositely directed to that of the iron, and the quoted error is primarily associated with the error in k. This value for μ_{Mo} compares well with the neutron-diffraction results of $-0.1\pm0.6\mu_B$ (Ref. 6) and $-0.6\pm0.6\mu_B$.[7] If the iron atoms were assumed to carry an average moment of $2.22\mu_B$ independent of C, one would calculate $\mu_{\mathrm{Mo}}=+0.1\pm0.05\mu_B$ from the saturation-magnetization results.

A further comparison with the neutron-diffraction results can be made by using the empirical constants of Bernas and Campbell[8] to calculate ΔH. The resultant $\Delta H/H_{\mathrm{Fe}}$ for *Fe*Mo of 8.0% is in rather poorer agreement with the measured 12% than the other examples cited by Bernas and Campbell. This may be due to the fact that Campbell's analysis of the neutron-diffraction data for *Fe*Mo was made before the value of $d\bar{\mu}/dC$ became available and the derived moment distribution would be expected to be somewhat altered from the published results[7] were this taken into account.

The authors are indebted to M. E. Fine and M. V. Nevitt for stimulating discussions and to A. Aldred for permission to use his unpublished magnetization data.[12]

[12] A. Aldred (private communication).

PHYSICAL REVIEW VOLUME 162, NUMBER 2 10 OCTOBER 1967

Jahn-Teller Effect of a d^1 Ion in Eightfold Cubic Coordination*

U. T. Höchli
Texas Instruments Incorporated, Dallas, Texas
(Received 17 May 1967)

The paramagnetic resonance of $Sc^{2+}(3d^1)$ exhibits three different kinds of spectra as the temperature is raised from 1.5 to 77°K. They are all explained in terms of internal asymmetry due to electronic-vibrational coupling (Jahn-Teller effect). Quantum-mechanical tunneling, as well as relaxation and strain, have an effect on the paramagnetic-resonance transitions. The first two effects are used to determine the symmetry and the energy level of the lowest vibronic states. From this an estimate of the parameters which describe the Jahn-Teller potential is made.

I. INTRODUCTION

THE dependence of paramagnetic resonance spectra of impurities in solids on the direction of the external magnetic field reflects the local symmetry near the impurity. For impurities substituting for lattice ions the local symmetry is very often the same as the crystal symmetry. This relationship is modified in two instances. First, another defect can be associated with the impurity. The resulting descent in symmetry is then found by considering all symmetry elements which leave both the impurity and the associated defect invariant. Second, the electronic state can be coupled to nuclear vibrations to yield a descent in symmetry. This much less obvious case is called the Jahn-Teller effect and is the subject of numerous publications.[1–4] It is of importance only when the electronic state has an orbital degeneracy of two or more which arises from the crystalline field. Such cases have been investigated by paramagnetic resonance.[5–7]

Recently the system $MgO:Cu^{2+}$ attracted special interest. The ground state of $Cu^{2+}(3d^9)$ in octahedral coordination is Γ_3. A theoretical study of d^9 ions in octahedral symmetry was undertaken by Bersuker

* This research in part sponsored by Air Force Office of Scientific Research Contract No. F 44620-67-C-0073.

[1] H. A. Jahn and E. Teller, Proc. Roy. Soc. (London) **161**, 220 (1937).
[2] J. H. Van Vleck, J. Chem. Phys. **7**, 72 (1939).
[3] V. Öpik and M. H. L. Pryce, Proc. Roy. Soc. (London) **A238**, 425 (1957).
[4] M. C. M. O'Brien, Proc. Roy. Soc. (London) **A281**, 323 (1964).
[5] A. Abragam and M. H. L. Pryce, Proc. Roy. Soc. (London) **A206**, 164 (1951).
[6] B. Bleaney, K. O. Bowers, and R. S. Trenam, Proc. Roy. Soc. (London) **A228**, 157 (1955).
[7] S. Geschwind and J. P. Remeika, J. Appl. Phys. **33**, 370 (1962) and references therein.

et al.,[8,9] who explained the temperature variation of the g factor previously observed in Ref. 6. They could also predict more features of the spectra which we will discuss later. A more recent piece of information, which supports Bersuker's model which involves tunneling between equivalent states, is an observation by Coffman.[10] He found that the electron paramagnetic resonance (EPR) of $MgO:Cu^{2+}$ exhibits anisotropic cubic symmetry and he tentatively ascribed part of his spectra to Bersuker's tunneling model. The presence of many other impurities in MgO and the linewidth of the Cu lines of 10 to 20 G made a more detailed analysis difficult.

The systems studied in this paper, $CaF_2:Sc^{2+}$ and $SrF_2:Sc^{2+}$, lend themselves nicely to a quantitative analysis of the tunneling model for several reasons: (1) CaF_2 and SrF_2 are available in high enough purity so nothing obscures the Sc spectra, and (2) the lines are narrow enough so that the orbital g shifts can easily be determined and both hyperfine interaction with Sc and F can be resolved. The ground state of $Sc^{2+}(3d^1)$ in eightfold coordination is Γ_3, same as for $MgO:Cu^{2+}$. The only difference between the two systems is the sign of the spin-orbit coupling. For Cu^{2+} the orbital contribution to the g factor is positive, thus $g \geq 2$, whereas for Sc^{2+}, it is negative, $g \leq 2$. Other than that the two systems are equivalent.

The purpose of this paper is fourfold. (1) It will be shown that Sc^{2+} in fluorites is a transition metal ion, isoelectronic to Ti^{3+}. (2) Since its orbital ground state is degenerate, Sc^{2+} is subject to a Jahn-Teller effect. Experimental data are presented which support the tunneling model. (3) The theory of Zeeman interaction within the tunneling model is extended to magnetic fields in arbitrary directions in order to check the model and allow the calculation of nuclear vibrational overlap. (4) Energy parameters are gained from the experiment. Their relative sizes are in agreement with the ordering of interactions according to their magnitude. For our system it turns out that the tunnel splitting is large compared to the Zeeman energy. Resonance is observed in both tunneling levels and its temperature dependence is in agreement with the model.

We proceed by qualitatively describing the tunneling model in Sec. II. This will serve as reference for Sec. III, where the theory of the tunneling model is briefly reviewed and extended to angular-dependent Zeeman interaction. Section IV is devoted to a presentation of the experimental data and their relationship to the model. In Sec. V some energy parameters describing the Jahn-Teller potential are deduced from the data.

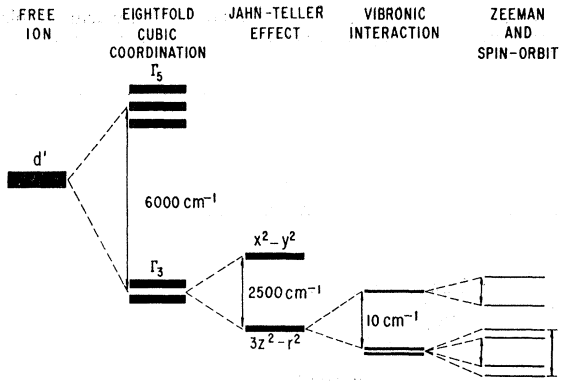

FIG. 1. Energy-level diagram of $CaF_2:Sc$.

They are used as a criterion for the validity of the theory.

II. THE TUNNELING MODEL

Sc^{2+} replaces Ca^{2+} in cubic CaF_2. The symmetric configuration of the complex ScF_8 is a cube, whose corners are occupied by fluorine nuclei and its body center by scandium. The orbital ground state of the d^1 electron bound to scandium is Γ_3, i.e., twofold degenerate. A quantitative analysis of the vibronic coupling of Γ_3 states by Öpik and Pryce[3] shows that the distortion will be along one of three fourfold $\langle 100 \rangle$ axes. They also predict that it will usually consist in an elongation along these axes; however, no use is made of this argument since the eigenvalues of the Zeeman operator are independent of the sign of the Jahn-Teller energy. For an elongation along the z axis the two orbitals for a d^1 electron are

$$(1/\sqrt{3})(3z^2-r^2)f(r) \quad \text{and} \quad (x^2-y^2)f(r).$$

They are split, the first being lower in energy (see Fig. 1). It is important to note that there are three equivalent distortions, denoted by elongations X, Y, and Z. Each is accompanied by an orbital ground state. Neither the distortions nor the orbitals are linearly independent, e.g., the superposition of the static distortions equals zero and likewise the sum of the orbitals vanishes. An analogous situation is found for the NH_3 molecule where the nitrogen nucleus has two stable positions outside the H_3 plane. These can be expressed as distortions Z and $-Z$ of a "flat" NH_3 molecule. The consequences for the ammonia molecule have been studied in detail[11] and can be summarized as follows. Once tunneling is allowed between the two stable "distorted" configurations Z and $-Z$, the vibrational wave functions Ψ_Z and Ψ_{-Z} are no longer eigenfunctions. The correct choice of basis functions is

$$\Psi_{\text{sym}} = (1/\sqrt{2})(\Psi_Z + \Psi_{-Z})$$

and

$$\Psi_{\text{anti}} = (1/\sqrt{2})(\Psi_Z - \Psi_{-Z}),$$

[8] I. B. Bersuker, Zh. Eksperim. i Teor. Fiz. **43**, 1315 (1962); **44**, 1239 (1963) [English transls.: Soviet Phys.—JETP **16**, 933 (1963); **17**, 836 (1963).

[9] I. B. Bersuker and B. G. Vekhter, Fiz. Tver. Tela **5**, 2432 (1963) [English transl.: Soviet Phys.—Solid State **5**, 1772 (1964)].

[10] R. E. Coffman, Phys. Letters **19**, 475 (1965); **21**, 381 (1965).

[11] G. H. Townes and A. L. Schawlow, *Microwave Spectroscopy* (McGraw-Hill Book Company, Inc., New York, 1955), p. 300.

TABLE I. Equivalent stable configurations of ScF_8 and NH_3.

	ScF_8	NH_3
Symmetric configuration	Cubic (O_h)	Planar (D_{3h})
Stable configuration	Tetragonal (D_{4h})	Trigonal (C_{3v})
Number of stable configurations	3	2
Number of linearly independent distortions	2	1
Energy scheme	Singlet and doublet	Two singlets
Symmetrized wave functions:		
Symmetric	$(3-3\gamma)^{-1/2}(\Psi_1+\Psi_2+\Psi_3)$	$1/\sqrt{2}(\Psi_1+\Psi_2)$
"Antisymmetric"	$\left\{\begin{matrix}(2+\gamma)^{-1/2}(\Psi_1-\Psi_2)\\(6+3\gamma)^{-1/2}(-\Psi_1-\Psi_2+2\Psi_3)\end{matrix}\right\}$	$1/\sqrt{2}(\Psi_1-\Psi_2)$

i.e., symmetrized wave functions. The energy splitting I between these is given by $I\approx\hbar\omega'\gamma$. $\hbar\omega'$ is a vibrational quantum for a harmonic oscillation in one well and the vibrational overlap is γ, where

$$\gamma=\int_{-\infty}^{\infty}\Psi(Z)\Psi(-Z)dZ. \tag{1}$$

I is called the inversion splitting. Note that the symmetrized wave functions transform according to the irreducible representations of the inversion group whereas the original uncoupled functions Ψ_Z and Ψ_{-Z} do not.

The basic features of Jahn-Teller distorted ScF_8 are the same as those for NH_3, although the causes for the distortions are different. Starting with wave functions that denote a motion around a single stable configuration Ψ_x, Ψ_y, Ψ_z for ScF_8, or Ψ_Z and Ψ_{-Z} for NH_3, one allows for an overlap $\gamma_{ij}=\int\Psi_x\Psi_y dQ$ between equivalent degenerate wave functions and solves[12]

$$\det(H_{ij}-\gamma_{ij}E)=0, \tag{2}$$

where H_{ij} are matrix elements of the Hamiltonian described in the theoretical part of this paper. The eigenvalues for NH_3 are the well-known two inversion levels, for ScF_8 they are a singlet and a doublet omitting the spin. Their energy difference is called tunnel splitting. The new wave functions transform according to irreducible representations of D_{3h} for NH_3 and O_h for ScF_8. We call them the symmetrized wave functions. Table I gives a summary of the relations for these two cases. An energy diagram for the ScF_8 case is given in Fig. 1. Starting from a free d^1 ion, a cubic field of eightfold coordination is applied. This puts Γ_3 in the ground state and Γ_5 in the excited state separated by 10 Dq. A d^9 ion in sixfold coordination shows the same splitting. The electrostatic coupling between the Γ_3 orbital and ligand nuclei distorts the nuclear configuration so that Γ_3 is split into $3z^2-r^2$ and x^2-y^2, the former being lower (Jahn-Teller effect). To each of the three equivalent fourfold axes there is one "ground" state. If quantum-mechanical tunneling is allowed between these equivalent states, a splitting is introduced. The wave functions transform according to the irreducible representation of the symmetry group S_3 (permutation of axes) which is isomorphous to C_{3v} and a subgroup of O_h. Consequently, the states are labeled Γ_k, $k=1, 2, 3$. The index k plays the same role as parity in the case of NH_3; the inversion group is isomorphous to S_2. Finally, the spin is included and an external magnetic field is applied. This splits the vibronic levels as indicated on the right side of Fig. 1.

The concept of an energy barrier between equivalent distortions of ScF_8 may present some difficulties in understanding. For the NH_3 case the meaning is obvious. The potential for the motion of the nitrogen atom in the Z direction is given by $V(Z)$, which has minima for Z_0 and $-Z_0$ and a maximum for $Z=0$. The energy barrier $E_b=V(0)-V(Z_0)$. The corresponding diagram for ScF_8 is three dimensional. We choose the normal coordinates Q_2 and Q_3[2,13] as basis for the distortions X, Y, and Z and have $Z=Q_2$, $X=-\frac{1}{2}Q_2+(\sqrt{3}/2)Q_3$, $Y=-\frac{1}{2}Q_2-(\sqrt{3}/2)Q_3$. The energy as a func-

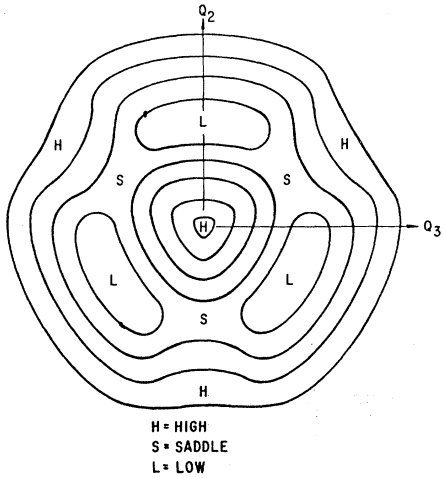

FIG. 2. Energy map in distortion space Q_2-Q_3.

[12] H. Eyring, J. Walter, and G. E. Kimball, *Quantum Chemistry* (John Wiley & Sons., Inc., New York, 1957), p. 193.

[13] A. D. Liehr and C. J. Ballhausen, Ann. Phys. (N.Y.) **3**, 304 (1958).

tion of these normal coordinates is mapped in Fig. 2. The motion of the complex will occur on a circle $\rho^2=Q_2^2+Q_3^2$ and the potential can be expressed as function of $\beta=\tan^{-1}(Q_2/Q_3)$. The saddle points then become maxima in β space and the energy barrier $V_0=E(S)-E(L)$. With $H(=\text{high})$ denoting the symmetric configuration, we call $E(H)-E(L)$ the stabilization energy. The potential $V(\beta)$ has three minima and is cyclic. Thus, if the kinetic energy of the nuclei is sufficient to overcome the energy barrier, their motion can be regarded as a hindered rotation in β space. This is why we call the eigenstates of the high-temperature Jahn-Teller-effect rotational states. Whereas in early papers the term "dynamical Jahn-Teller effect" was mainly used to describe the motional averaging of *EPR* spectra, it is now[14] also used to describe transitions due to quantum-mechanical tunneling between distorted configurations.

The relation between the tunnel splitting and internal random strain determines whether a static or a dynamic Jahn-Teller effect is observed at 0°K using sufficiently small microwave frequencies. If at the site of an impurity a tetragonal field in the Z direction is superimposed to the cubic field, one vibronic function, $Z(3z^2-r^2)$ assumes a lower energy than the other two, say $-\delta_s$. If $|\delta_s|>3\Gamma$, there is little probability for the complex to be oriented in any other than the Z direction. Therefore, it behaves just like a center of axial symmetry along the Z axis. Because of its random character the strain will produce an equal amount of X, Y, and Z centers. In the present case, however, $3\Gamma<|\delta_s|$, all our data can be explained without involving strain.

In order to observe transitions within tunneling levels by EPR it is necessary that the characteristic tunneling frequency be larger than the difference in Larmor frequency, i.e., $3\Gamma/h>\Delta g\beta_e H/h$, where Δg is the g anisotropy, 3Γ the tunnel splitting, h Planck's constant, β_e the Bohr magneton of the electron, and H the external magnetic field. If this condition is not satisfied, i.e., if tunneling slow compared to Larmor precession, the complex can be considered localized in one well during a microwave transition. Consequently axial spectra should be observed. In principle it should be possible to find a transition from a dynamic to a static Jahn-Teller effect by merely raising the microwave frequency above $\nu_t=3\Gamma/4u\hbar$, where the quantity $4u=4\lambda/10Dq=\bar{g}-2$ will be introduced later. In our case it turns out that $\nu_t\sim6000$ GHz, corresponding to a wavelength of $\lambda\sim0.05$ mm, preventing the determination of 3Γ by this method.

III. THEORY

The Hamiltonian for a single d electron coupled to nine nuclei forming the ScF_8 complex is given by

$$H=H_e+H_n+H_{en}. \tag{3}$$

The Hamiltonian for the electron is

$$H_e=\sum_k(\hbar^2/2m_e)\partial^2/\partial q_k^2+V(q_k, Q_{k0}), \tag{4}$$

where V accounts for the static electric field caused by the ligands, q_k are electronic coordinates and Q_{k0} are the nuclei in their unperturbed positions. The solutions are the well-known d orbitals in a cubic field. The Hamiltonian for the nuclear part expressed in terms of normal coordinates of the nuclei is given by

$$H_n=\sum_k(\omega^2Q_k^2+P_k^2), \tag{5}$$

where $P_k=\partial/\partial\dot{Q}_k$. The solutions are oscillators for each normal coordinate. The coupling term H_{en} accounts for the change of energy the orbitals receive due to displacement of the ligands. It is expanded in a Taylor series in Q_k and the linear term is retained:

$$H_{en}=\sum_k V_kQ_k, \tag{6}$$

where $V_k=\partial V/\partial Q_k$ is a coupling coefficient describing the sensitivity of the electronic wave function to a displacement of the ligands.

Jahn and Teller pointed out that this coupling term linear in Q_k acting between degenerate wave functions causes the energy of the vibrational-electronic wave function to depend linearly on Q_k. Since V_kQ_k is the only linear term determining the perturbation energy, the configuration $Q_k=0$ cannot represent an energy minimum. Instead a stable configuration is reached where the elastic energy balances out the coupling term, i.e., for

$$(\partial/\partial Q_k)(\alpha Q_k^2+V_kQ_k)=0. \tag{7}$$

This is the case for

$$Q_{kt}=-V_k/2\alpha \tag{8}$$

and shows that the static distortion of ScF_8 increases with the strength of coupling between the d electron and the nuclear complex. A detailed quantitative description of this situation has been given by Öpik and Pryce,[3] and Liehr and Ballhausen.[13]

The symmetry of the ground state Γ_3 eliminates most of the coupling terms, since in a cubic crystal any nonzero quantity must transform according to the irreducible representation Γ_1 of the cubic group. The expectation value of V_kQ_k given by

$$\langle V_kQ_k\rangle-\langle\varphi_e, V_kQ_k\varphi_e'\rangle \tag{9}$$

transforms according to $(\Gamma_3\times\Gamma_i\times\Gamma_3)_s$. Γ_i is the irreducible representation for the nuclear normal coordinates. If the product representation contains Γ_1, then $i=1$ or 3. For $i=1$ the coupling term has the same symmetry as the elastic term Q_k^2 and therefore does not contribute to the linear term in the coupling. For $i=3$ the normal coordinates for cubic coordination are given by Liehr,[15] who uses the symbols S_{2b} and S_{2a}.

[14] F. S. Ham, Phys. Rev. **138**, 1727 (1965).

[15] A. D. Liehr, in *Progress in Inorganic Chemistry*, edited by Frank A. Cotton (Interscience Publishers, Inc., New York, 1961), Vol. 3, p. 302.

TABLE II. Symmetrized-vibronic wave functions of Γ_6 and Γ_8 states in cubic symmetry.[a]

Elongated cubes

$$\Psi_s^+=(3-3\gamma)^{-1/2}[u^+(Z-\tfrac{1}{2}Y-\tfrac{1}{2}X)-\tfrac{1}{2}\sqrt{3}v^+(X-Y)+d\{(\tfrac{1}{2}i)a^-(X-Z)+(\tfrac{1}{2}b^-)(Y-Z)+(\tfrac{1}{2}ic^+)(Y-X)\}],$$

$$\Psi_1^+=(2+\gamma)^{-1/2}[\tfrac{1}{2}u^+(Y-X)-(\tfrac{1}{2}\sqrt{3})v^+(X+Y)+d\{-(\tfrac{1}{2}\sqrt{3})ic^+(X+Y)+(\tfrac{1}{2}i\sqrt{3})a^-X-(\tfrac{1}{2}i\sqrt{3})b^-Y\}],$$

$$\Psi_2^+=(6+3\gamma)^{-1/2}[u^+(\tfrac{1}{2}X+\tfrac{1}{2}Y+2Z)+(\tfrac{1}{2}\sqrt{3})v^+(X-Y)+d\tfrac{1}{2}\sqrt{3}\{-ia^-(X+2Z)-ib^-(Y+2Z)+ic^+(X-Y)\}].$$

Shortened cubes

$$\Psi_s^+=(3-3\gamma)^{-1/2}[\tfrac{1}{2}v^+(-X-Y+2Z)+(\tfrac{1}{2}\sqrt{3})u^+(-X+Y)+d\{ia^-(X-\tfrac{1}{2}Y-\tfrac{1}{2}Z)+b^-(\tfrac{1}{2}X-Y+\tfrac{1}{2}Z)+ic^+(-\tfrac{1}{2}X-\tfrac{1}{2}Y+Z)\}].$$

$$\Psi_1^+=(2+\gamma)^{-1/2}[-\tfrac{1}{2}v^+(X-Y)-(\tfrac{1}{2}\sqrt{3})u^+(X+Y)+d\{-ic^+(\tfrac{1}{2}X-\tfrac{1}{2}Y)+b^-(\tfrac{1}{2}X+Y)+ia^-(X+\tfrac{1}{2}Y)\}],$$

$$\Psi_2^+=(6+3\gamma)^{-1/2}[\tfrac{1}{2}v^+(X+Y+4Z)+(\tfrac{1}{2}\sqrt{3})u^+(X-Y)+d\{ic^+(\tfrac{1}{2}X+\tfrac{1}{2}Y+2Z)+b^-(-\tfrac{1}{2}X+Y+Z)+ia^-(-X+\tfrac{1}{2}Y-Z)\}].$$

[a] Ψ^- is obtained from Ψ^+ by changing all spin signs and replacing b with $-b$ and c with $-c$. The indices s, 1, and 2 stand for Γ_6, Γ_8, and Γ_8'. The orbitals are

$$v=(1/\sqrt{3})(3z^2-r^2)f(r),$$
$$u=(x^2-y^2)f(r),$$
$$a=2yzf(r),$$
$$b=2xzf(r),$$
$$c=2xyf(r).$$

Z denotes the vibrational wave function

$$Z=\chi(Z)=\chi(Q_2),$$
$$X=\chi(-\tfrac{1}{2}Q_2+\tfrac{1}{2}\sqrt{3}Q_3),$$
$$Y=\chi(-\tfrac{1}{2}Q_2-\tfrac{1}{2}\sqrt{3}Q_3).$$

Even though the normal coordinates S_{2b}, S_{2a} for the cubic case and Van Vleck's Q_2, Q_3 for the octahedral case take a different form if expressed in terms of nuclear displacements, they are equivalent. Both S and Q describe a tetragonal elongation T_z of a cube, or an octahedron, respectively, along a fourfold z axis. The relation between distortions and normal coordinates is given by

$$\begin{aligned}T_z&=Q_2,\\ T_x&=-\tfrac{1}{2}Q_2+\tfrac{1}{2}\sqrt{3}Q_3,\\ T_y&=-\tfrac{1}{2}Q_2-\tfrac{1}{2}\sqrt{3}Q_3.\end{aligned}\tag{10}$$

All three distortions T_x, T_y, and T_z are equivalent. The values for static equilibria are labeled by Q_{2t} and Q_{3t}. The zero-point vibrational wave functions expressed in these coordinates are

$$\begin{aligned}Z&=\prod_{k=1,4,5\cdots p}\chi_{nk}(Q_k)\chi(Q_2-Q_{2t}),\\ X&=\prod_{k=1,4,5\cdots p}\chi_{nk}(Q_k)\chi[-\tfrac{1}{2}(Q_2-Q_{2t})+\tfrac{1}{2}\sqrt{3}(Q_3-Q_{3t})],\\ Y&=\prod_{k=1,4,5\cdots p}\chi_{nk}(Q_k)\chi[-\tfrac{1}{2}(Q_2-Q_{2t})-\tfrac{1}{2}\sqrt{3}(Q_3-Q_{3t})].\end{aligned}\tag{11}$$

We label them Z, X, and Y since they represent oscillations around static tetragonal distortions in the z, x, and y direction. We disregard other oscillations because they do not couple to the electron. According to the adiabatic principle the electrons adjust instantaneously assuming the orbitals $3z^2-r^2$, $3x^2-r^2$, $3y^2-r^2$. The application of the adiabatic principle to degenerate wave functions is a generalization[16] of the Born-Oppenheimer[17] approximation. The total vibronic-zero-order wave functions describing the decoupled stable equilibrium states are

$$\begin{aligned}\Psi_1&=X(3x^2-r^2),\\ \Psi_2&=Y(3y^2-r^2),\\ \Psi_3&=Z(3z^2-r^2).\end{aligned}\tag{12}$$

If these wave functions are orthogonal, they are degenerate in the sense that they have the same energy and transform into each other under operations of the cubic group. We call this sort of degeneracy equivalence degeneracy.

The next step is to allow for overlap between pairs of wave functions and to symmetrize them according to the recipe given in Sec. II. The result is

$$\begin{aligned}\Psi_s'&=(3-3\gamma)^{-1/2}(\Psi_1+\Psi_2+\Psi_3),\\ \Psi_1'&=(2+\gamma)^{-1/2}(\Psi_1-\Psi_2),\\ \Psi_2'&=(6+3\gamma)^{-1/2}(-\Psi_1-\Psi_2+2\Psi_3),\end{aligned}\tag{13}$$

for the wave function and

$$\begin{aligned}E_s'&=2\Gamma,\\ E_1'&=E_2'=-\Gamma,\end{aligned}\tag{14}$$

for the energies. 3Γ is the tunnel splitting. Finally we want to include the action of the spin-orbit coupling. To do this, we correct our orbitals $3z^2-r^2$ and x^2-y^2 by

$$\begin{aligned}\sqrt{3}\varphi_1&=3z^2-r^2+\sum_\rho \lambda/\Delta<3z^2-r^2/\mathbf{L}\cdot\mathbf{S}/\rho>\rho,\\ \varphi_2&=x^2-y^2+\sum_\rho \lambda/\Delta<x^2-y^2/\mathbf{L}\cdot\mathbf{S}/\rho>\rho,\end{aligned}\tag{15}$$

where ρ denotes any orbital of the excited Γ_5 state. This does not have any effect on the symmetry of the resulting wave functions. This is readily verified by checking their transformation properties under the double group. The unperturbed wave functions trans-

[16] H. C. Longuet-Higgins, *Advances in Spectroscopy 2* (Interscience Publishers, Inc., New York, 1961), p. 429.
[17] M. Born and R. Oppenheimer, Ann. Physik **84**, 457 (1927).

form as $\Gamma_3\times\Gamma_6=\Gamma_8$. Since the spin-orbit coupling $\mathbf{L}\cdot\mathbf{S}$ transforms as Γ_1, the ground state couples only the part of the excited state transforming according to Γ_8 and the first-order wave functions also transform as Γ_8. Thus we expect our spectra to exhibit cubic symmetry, instead of axial, as is found for the static Jahn-Teller effect. The conservation of symmetry is the main feature which distinguishes a dynamical Jahn-Teller effect from the static Jahn-Teller effect. The symmetrized wave functions are given in Table II for both d^1 and d^9 in elongated cubes. The d^1 wave functions for shortened cubes are the same as the d^9 wave functions for elongated cubes. They likewise have cubic symmetry. The wave functions for d^1 check with those evaluated by Bersuker[8] for d^9 in elongated octahedra, as they should.

The Zeeman operator

$$Z'=\beta\mathbf{H}(g_0\mathbf{S}+\mathbf{L}), \tag{16}$$

expressed in terms of this basis leads to a 4×4 matrix for the quartet Γ_8 state and a 2×2 matrix for the doublet Γ_6 state. We can safely neglect cross terms between Γ_6 and Γ_8, since $\Delta g\beta H/3\Gamma\sim10^{-4}$. The result for the quartet Γ_8 state is similar to that obtained for a Γ_8 state in the limit of strong spin-orbit coupling[5] (no Jahn-Teller effect). It differs quantitatively by factors of $-\frac{1}{2}$ and $1+\frac{3}{2}\gamma$, where $-\frac{1}{2}$ represents electronic and γ the vibrational overlap. For the magnetic field in a (010) plane the Zeeman operator becomes

$$Z'=\beta(H_xL_x+H_zL_z+g_0H_xS_x+g_0H_zS_z). \tag{17}$$

Putting $H_x=Hl$, $H_z=Hn$, where l and n are directions cosines, and $\lambda/\Delta=d$, we obtain the following results:

$$(\beta H)^{-1}Z=\begin{array}{c} \begin{matrix} s^+ & s^- \end{matrix} \\ \begin{bmatrix} n+2nd & l+2ld \\ l+2ld & -n-2nd \end{bmatrix} \end{array} \tag{18}$$

for the doublet Γ_6 state and

$$(\beta H)^{-1}Z=\begin{array}{c} \begin{matrix} a^+ & b^+ & a^- & b^- \end{matrix} \\ \begin{bmatrix} n+nd(1-\frac{3}{2}\gamma) & 0 & l+ld(\frac{5}{2}+\frac{3}{4}\gamma) & -\frac{1}{2}\sqrt{3}ld(1+\frac{3}{2}\gamma) \\ 0 & n+3nd(1+\frac{1}{2}\gamma) & -\frac{1}{2}\sqrt{3}ld(1+\frac{3}{2}\gamma) & l+ld(\frac{3}{2}-\frac{3}{4}\gamma) \\ l+ld(\frac{5}{2}+\frac{3}{4}\gamma) & -\frac{1}{2}\sqrt{3}ld(1+\frac{3}{2}\gamma) & -n-nd(1-\frac{3}{2}\gamma) & 0 \\ -\frac{1}{2}\sqrt{3}ld(1+\frac{3}{2}\gamma) & l+ld(\frac{3}{2}-\frac{3}{4}\gamma) & 0 & -n-3nd(1+\frac{1}{2}\gamma) \end{bmatrix} \end{array} \tag{19}$$

for the quartet Γ_8 state. The indices $+$ and $-$ represent the spin quantum number $+\frac{1}{2}$ and $-\frac{1}{2}$.

It is more convenient to transform the basis functions, so that the spin is quantized in the direction of the magnetic field. The transformation is given by

$$\varphi_1=\frac{l}{(2-2n)^{1/2}}\varphi_+ + \frac{1-n}{(2-2n)^{1/2}}\varphi_-,$$

$$\varphi_2=-\frac{1-n}{(2-2n)^{1/2}}\varphi_+ + \frac{l}{(2-2n)^{1/2}}\varphi_-, \tag{20}$$

and the matrix, expressed in the new basis, becomes

$$(\beta H)^{-1}Z_s''=\begin{bmatrix} 1+2d & 0 \\ 0 & -(1+2d) \end{bmatrix}. \tag{21}$$

$\beta H^{-1}Z''\equiv Z_{ik}=Z_{ki}$, where

$$\begin{aligned} Z_{11}&=-Z_{33}=1+2d+d(n^2-\tfrac{1}{2}l^2)(1+\tfrac{3}{2}\gamma), \\ Z_{22}&=-Z_{44}=1+2d-d(n^2-\tfrac{1}{2}l^2)(1+\tfrac{3}{2}\gamma), \\ Z_{14}&=Z_{23}=\tfrac{3}{2}dnl(1+\tfrac{3}{2}\gamma), \\ Z_{12}&=Z_{34}=\tfrac{1}{2}\sqrt{3}dl^2(1+\tfrac{3}{2}\gamma), \\ Z_{13}&=Z_{24}=0. \end{aligned} \tag{22}$$

An excellent approximate solution can be obtained by neglecting the elements Z_{14} and Z_{23}, which couple states that are separated by βH. The error incurred is quadratic in d. This amounts to decoupling the two antisymmetric states and quantizing each orbital momentum $\beta H\lambda/\Delta$ separately in the direction of the applied magnetic field. The result is for the quartet Γ_8 state

$$\begin{aligned} E_1&=-E_3=1+2d\pm d(1+\tfrac{3}{2}\gamma)(n^4+l^4-n^2l^2)^{1/2}, \\ E_2&=-E_4=-1-2d\pm d(1+\tfrac{3}{2}\gamma)(n^4+l^4-n^2l^2)^{1/2}, \end{aligned} \tag{23a}$$

and for the doublet Γ_6 state

$$E_s=\pm(1+2d). \tag{23b}$$

The g factors are

$$\begin{aligned} g_{1,2}&=2+4d\pm2d(1+\tfrac{3}{2}\gamma)(n^4+l^4-n^2l^2)^{1/2}, \\ g_s&=2+4d. \end{aligned} \tag{24}$$

The generalization to the case where the magnetic field is in a completely arbitrary direction is obvious. The only way to retain cubic symmetry is to put

$$\begin{aligned} g_{1,2}=2+4d\pm2d(1+\tfrac{3}{2}\gamma) \\ \times(n^4+l^4+m^4-n^2l^2-n^2m^2-m^2l^2)^{1/2}. \end{aligned} \tag{25}$$

The same g factors are obtained for flattened octahedra. The Zeeman effect is independent of the sign of the

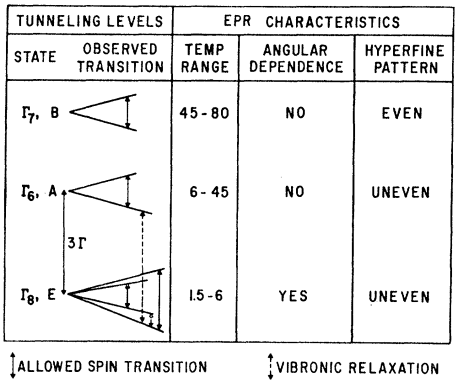

FIG. 3. Tunneling levels and corresponding EPR characteristics.

vibronic coupling. For H along $\langle 111\rangle$ the g factor becomes

$$g\langle 111\rangle = 2+4d, \tag{26}$$

which is equal to both the g factor of the doublet Γ_6 state and the rotational state. Furthermore, it is the average of the two g factors along $\langle 100\rangle$, $2+6d+3\gamma$, and $2+2d-3\gamma$.

Since the tunnel splitting can be estimated experimentally it is given here in terms of the parameters describing the Jahn-Teller potential. Using the WKB approximation one gets[18]

$$3\Gamma = \frac{3\hbar\omega'}{2\pi} \times \exp\left[-\frac{1}{2\hbar}\int_{[V-1/2\hbar\omega']>0}[2m(V(x)-\tfrac{1}{2}\hbar\omega')]^{1/2}dx\right]. \tag{27}$$

Using the potential

$$V=\tfrac{1}{2}V_0(1-\cos 3\theta), \tag{28}$$

one can carry out the integration for $2V_0 \gg h\omega'$:

$$3\Gamma=(3/2\pi)h\omega' \exp(-2V_0/h\omega'+1). \tag{29}$$

ω' is the characteristic frequency for the motion in β direction. It is approximately

$$\omega'=\omega\times\tfrac{3}{2}(V_0/E_{JT})^{1/2}, \tag{30}$$

where ω is the frequency of the ϵ_g mode in absence of the Jahn-Teller effect.

It will become clear from the experimental data that the relation $2V_0 \gg h\omega$ is not well satisfied, so any quantities deduced from the WKB approximation can only be used as a rough estimate of the Jahn-Teller potential. If the nuclear kinetic energy is increased above the barrier height, the nuclei rotate in β space. If the rotation frequency exceeds the difference in microwave frequency due to the g anisotropy the g factors and hyperfine constants become the average of the two extremes of the Γ_8 states.[5] Thus they are the same as for the symmetric state Γ_6.

The tunneling states can be influenced by strain. The energy change of the three states given by Eq. (12) due to strain is given by Ham[19]:

$$\begin{aligned}\Delta E_1&=-V(e_{xx}-\tfrac{1}{2}e_{yy}-\tfrac{1}{2}e_{zz}),\\ \Delta E_2&=-V(e_{yy}-\tfrac{1}{2}e_{zz}-\tfrac{1}{2}e_{xx}),\\ \Delta E_3&=-V(e_{zz}-\tfrac{1}{2}e_{xx}-\tfrac{1}{2}e_{yy}).\end{aligned} \tag{31}$$

Matrix elements of strain coupling different states are proportional to the overlap between these states and are neglected. The Hamiltonian including tunneling and strain becomes

$$H=\begin{bmatrix}-V(e_{xx}-\frac{1}{2}e_{yy}-\frac{1}{2}e_{zz}) & \Gamma & \Gamma\\ \Gamma & -V(e_{yy}-\frac{1}{2}e_{zz}-\frac{1}{2}e_{xx}) & \Gamma\\ \Gamma & \Gamma & -V(e_{zz}-\frac{1}{2}e_{xx}-\frac{1}{2}e_{yy})\end{bmatrix}. \tag{32}$$

If the strain energies are small, $V\,|\,e\,| \ll 3\Gamma$, the eigenstates are those of the tunneling Hamiltonian, as given by Eqs. (13) and (14). If the strain is large compared to the tunnel splitting, then the eigenstates are Ψ_1, Ψ_2, and Ψ_3, corresponding to a static Jahn-Teller effect. In the intermediate case the eigenvalues are given by

$$\begin{aligned}&E=\tfrac{1}{2}Ve_{zz}-\Gamma,\\ &E=-\tfrac{1}{4}Ve_{zz}+\tfrac{1}{2}\Gamma\pm[(\tfrac{1}{4}Ve_{zz}+\tfrac{3}{2}\Gamma)^2+\tfrac{1}{2}V^2e_{zz}]^{1/2},\end{aligned} \tag{33}$$

provided $e_{xx}=e_{yy}=0$.

IV. EXPERIMENTAL RESULTS

Sample Preparation

Cleaved crystals of CaF_2 and SrF_2, about 2 mm in diameter, were plated with Sc metal by condensation from Sc vapor. These samples were then held in a vacuum at 1200°C for 36 h to allow for diffusion of Sc into the host crystal. A Sc concentration of about 120 ppm for CaF_2 and 30 ppm for SrF_2 was obtained.

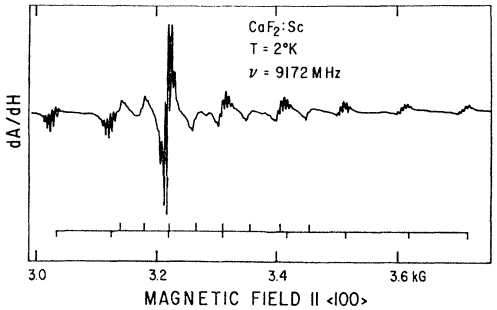

FIG. 4. EPR spectrum of $CaF_2:Sc^{2+}$ at 1.5°K with $H \parallel \langle 100\rangle$.

[18] M. D. Sturge (to be published).

[19] F. S. Ham (unpublished).

The same technique applied to CdF_2 and BaF_2 was unsuccessful. We believe that Sc introduced into CaF_2 and SrF_2 has a valence state of Sc^{3+} since no EPR could be detected. In this respect Sc behaves like a rare earth[20] which is almost invariably found in a 3+ state. X irradiation at room temperature converts Sc^{3+} to Sc^{2+}, which is found at a cubic site. X irradiation of $CaF_2:Sc^{3+}$ at 77°K does not produce a detectable amount of Sc^{2+}. CaF_2:Sc is of greyish color and slightly less transparent than pure CaF_2. The lack of any optical data is probably due to the low Sc concentration obtained.

Apparatus

Paramagnetic resonance data were obtained on a superheterodyne x-band spectrometer with single-band detection at 30 MHz. Since the lines did not saturate at any available power level, the spectrometer was run near optimum sensitivity of 2×10^{10} spins at $\rho_0=$ 0.01 mW, $T=1.5$°K, and a time constant of 1 sec. It was estimated that at least 10% of the Sc centers were detected indicating a reasonably effective conversion of Sc^{3+} into Sc^{2+} by x rays. Some additional data were obtained on a K-band homodyne spectrometer.

Data

This is the first report on paramagnetic data taken on scandium. Our model implies, and we will present experimental evidence, that the spectra are due to Sc^{2+} substitutional for the cation in CaF_2 and SrF_2. Since neutral Sc has the configuration $(Ar)3d^24p^1$, Sc^{2+} can have either a $3d$ or a $4s$ electron unpaired. However, the anisotropy seen in the spectra at low temperature and the transition to an isotropic spectrum at high temperature prove the presence of a Jahn-Teller effect and rule out paramagnetism due to a $4s$ electron. Scandium behaves therefore like a normal transition metal ion and is isoelectronic to Ti^{3+}. Since its configuration is so simple, it should be possible to get unambiguous information from other systems doped with Sc^{2+}.

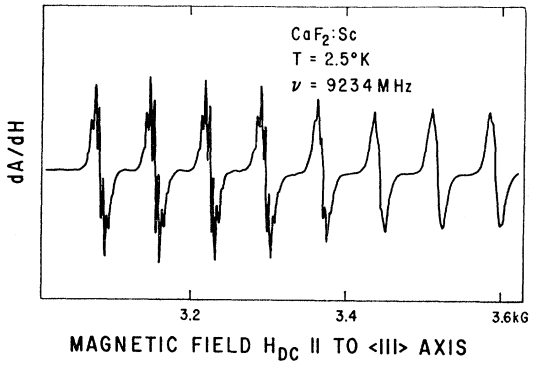

FIG. 5. EPR spectrum of $CaF_2:Sc$, $H \parallel \langle 111\rangle$.

[20] B. Bleaney, P. M. Llewellyn, and D. A. Jones, Proc. Phys. Soc. (London) **69**, 858 (1956).

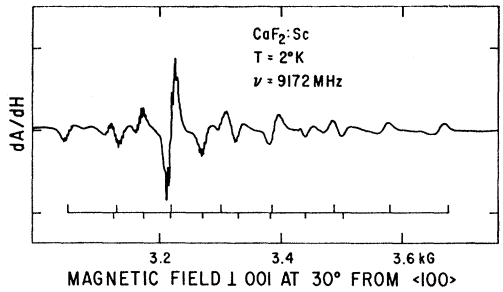

FIG. 6. EPR spectrum of $CaF_2:Sc$, $H \parallel \langle 110\rangle$, X band.

There are three temperature regions in each of which one characteristic spectrum is observed (Fig. 3). Between 1.5 and 6°K an anisotropic spectrum consisting of two electronic transitions is observed. Each of them is split into 8 almost equidistant lines due to interactions with the Sc^{45} nucleus. Its hyperfine components show a specific uneven amplitude distribution. We attribute this spectrum to the two allowed transitions of the Γ_8 state. Between 6 and 45°K an isotropic spectrum is observed. It also has an uneven amplitude distribution which becomes more and more even at the upper end of the temperature range. It is attributed to the one allowed transition within the symmetric state (Γ_6). Above 45°K the amplitude distribution of this transition is even and the lines broaden beyond detection at 80°K.

We now proceed to a more detailed discussion of the three spectra. The EPR spectra taken at 1.5°K with the magnetic field along a $\langle 100\rangle$, a $\langle 111\rangle$, and a $\langle 110\rangle$ axis are given in Figs. 4, 5, and 6. All spectra show a well resolved $I=\frac{7}{2}$ hyperfine structure due to the interaction of the d electron with the Sc^{45} nucleus. Furthermore, a partially resolved structure is seen which arises from an interaction with the eight ligand fluorines of $I=\frac{1}{2}$.

Care has to be taken in evaluating the g factor anisotropy and hyperfine structure. At first glance it might look as if Figs. 4, 5, and 6 represent a superposition of three axial centers of $\langle 100\rangle$ symmetry. Especially the fact that along $\langle 111\rangle$ all the centers are equivalent is misleading. A closer analysis shows, however, at least two pieces of information that are incompatible with the explanation involving axial centers. If the magnetic field H is parallel to [110], one spectrum should be perpendicular, namely [001]. This same spectrum should also arise with twice the intensity for $\mathfrak{C}\|[100]$, but does not. The definite disproof was obtained by taking data with the magnetic field in a (001) plane but not parallel to either [100] or [010]. Such a display is given in Fig. 7 where only two spectra are seen instead of the three predicted by the axial model.

The two observed spectra correspond to the two allowed transitions within the Γ_8 quartet described in the previous section. In Fig. 8 the experimental g factors are plotted as a function of the angle of the applied magnetic field with the [100] axis. They are compared with the theoretical values that are obtained

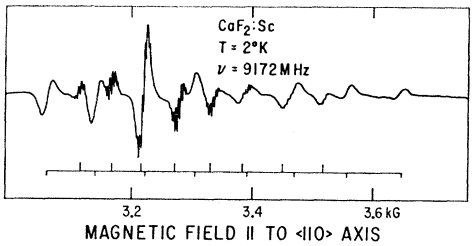

FIG. 7. EPR spectrum of CaF_2:Sc, $H \parallel \langle 120 \rangle$.

by fitting the parameters λ/Δ' and γ to the two g factors parallel to [100]. At $T=1.5°K$, $\lambda/\Delta'=(74\pm2)\cdot10^{-4}$ for CaF_2:Sc and $\lambda/\Delta'=(96\pm2)\times10^{-4}$ for SrF_2:Sc. $\Delta'=10Dq$ is the splitting between the Γ_3 and the Γ_5 orbitals. Together with the spin-orbit coupling constant of $\lambda=55$ cm^{-1} for the free Sc^{2+} we evaluate $\Delta'\leq7000$ cm^{-1} for CaF_2:Sc and $\Delta'\leq6000$ cm^{-1} for SrF_2:Sc. The inequality sign accounts for the fact that λ in a solid is smaller than in a free ion due to covalency. An experimental indication of this is the structure due to interaction of the d electron with the ligand fluorine. An optical transition is expected at $\geq14\,000$ Å but is not observed. The g factors and γ are given as a function of temperature in Fig. 9. A slight change in the g factors is observed at 5°K, for which we offer no explanation. The uncertainty in γ is too big to allow one to decide whether γ decreases with T or stays constant. We will make use of the fact that γ does not increase with T.

The hyperfine features have been studied more empirically. Transitions occur at

$$h\nu=g\beta H+KMm+K'^2/\beta H(I^2+I-M^2). \quad (34)$$

g, K, and K' are functions of the applied magnetic field. I, M, and m are the nuclear spin, its z component, and the electronic quantum number. The second-order hyperfine effect causes shifts in the order of 1 to 5 G, just slightly more than the experimental error. K has been taken as the average splitting of two adjacent hyperfine lines, K' was determined from the differences of the splittings. Then g was obtained from the empirical formula above. If instead the center of the pattern is

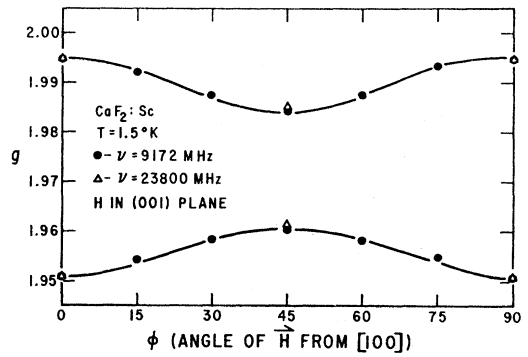

FIG. 8. g factors as a function of the direction of the applied magnetic field.

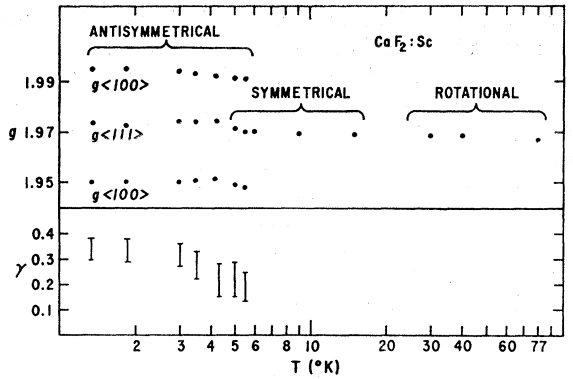

FIG. 9. g factors of the three different vibronic states of $CaF_2:Sc^{2+}$.

taken to obey $g\beta H=h\nu$, the resulting g factor deviates by only 10^{-3} from the correct one.

The hyperfine parameter K is given as a function of the direction of the applied field in Fig. 10. The same behavior is found as for g. Both g and K have cubic symmetry, i.e., they remain unchanged if direction cosines of the magnetic field with the crystalline axes are interchanged. g and K for the magnetic field along the principle axes are given in Table III. This behavior, typical for the dynamical Jahn-Teller effect, has been observed once before by Coffman[10] who gave it the name "third type of a Jahn-Teller effect."

The hyperfine splitting parameters K for all transitions, measured with the magnetic field along [100], can be fitted to Eq. (33) of Ref. 4. If terms in Q, which in a cubic field are of the order $d^2=(\lambda/10Dq)^2$, are neglected, then this equation reads

$$K/p=-\kappa-(4/7)\ \langle\cos\theta\rangle+(6/7)d\ \langle\cos\theta\rangle+g-2. \quad (35)$$

Here $p=2\gamma'\beta\beta_N\langle r^{-3}\rangle$ denotes the dipolar interaction and κ describes the admixture of unpaired s electrons to the ground-state configuration. γ' is the gyromagnetic ratio, β_N the nuclear magneton, and $\langle r^{-3}\rangle$ the one-electron average of r^{-3}. The average of $\cos\theta$ over Q_2-Q_3 space is $\pm\frac{1}{2}$ for Γ_8 transitions and vanishes for Γ_6 transitions. The set of data as shown in Table III yields three equations to determine p and κ. In order to avoid overdetermination, p and κ have been calcu-

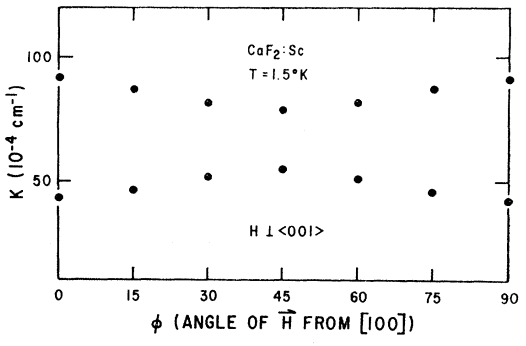

FIG. 10 Hyperfine splitting parameter as a function of the direction of the applied field.

TABLE III. g factors and hyperfine constants K for CaF_2:Sc and SrF_2:Sc. The data for the quartet Γ_8 states are taken at 1.5°K, for the symmetric states at 10°K, and for the rotational state at 77°K. Hyperfine constants are expressed in units of 10^{-4} cm^{-1}. The g factors are determined to an accuracy of 10^{-3} unless otherwise noted, and the hyperfine constants to about 0.5×10^{-4} cm^{-1}.

	CaF_2:Sc (f=9250 and 23800 MHz)		SrF_2:Sc (f=9250 MHz)	
	$H \parallel \langle 100\rangle$	$H \parallel \langle 110\rangle$	$H \parallel \langle 100\rangle$	$H \parallel \langle 110\rangle$
g_{a1}	1.951	1.961	1.936	1.950
g_{a2}	1.995	1.980	1.991	1.977
g_s	1.9688±5	1.9688±5	1.963	1.963
g_{rot}	1.967	1.967	not observed	
K_{a1}	89.5	76.6	91.2	78.7
K_{a2}	40.4	53.8	43.0	55.3
K_s	65.5	65.5	67.0	67.0
K_{rot}	65.0	65.0	not observed	

lated with the use of Γ_8 data only. Putting $\langle\cos\theta\rangle=\pm\frac{1}{2}$ in (35) and taking the g factor for a free electron $g_0=2.0023$ instead of 2, one finds

$$p=8.7\times10^{-3}\ \text{cm}^{-1},$$

$$\kappa=0.71.$$

One can now put $\langle\cos\theta\rangle=0$ and insert the values for p and κ in (35). The result $K(\Gamma_6)=65.0\cdot10^{-4}$ cm^{-1} checks with the corresponding experimental value of Table III, confirming consistency. Bleaney, Bowers, and Pryce[21] found both theoretically and experimentally that the unpaired spin density of a d^n ion at the nucleus almost is independent of the number of d electrons. They took as a measure of the unpaired spin density the quantity $\chi'=\lambda p/\gamma$. χ' ranges from

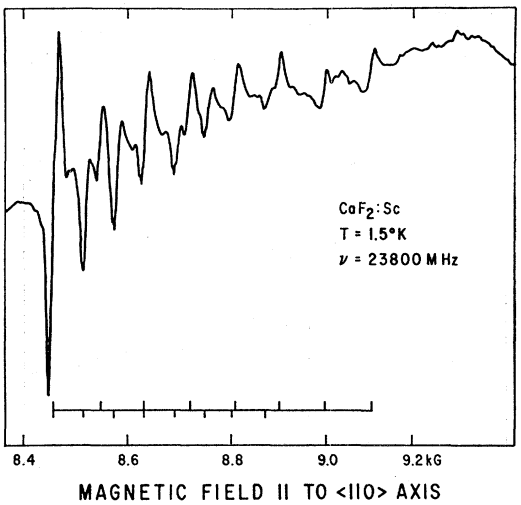

FIG. 11. EPR spectrum of CaF_2:Sc, $H \parallel \langle 110\rangle$, K band.

[21] B. Bleaney, K. D. Bowers, and M. H. L. Pryce, Proc. Roy. Soc. (London) **A228**, 166 (1955).

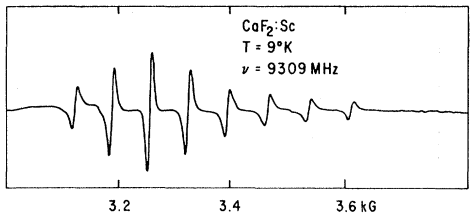

FIG. 12. EPR spectrum of CaF_2:Sc at 9°K. The symmetric state.

5.3 to 6.55×10^{-3} cm^{-1} for d^{2n+1} ions except Sc. Our value for Sc^{2+}, $\chi'=4.6\times10^{-3}$ cm^{-1}, confirms the validity of this view.

The superhyperfine structure due to ligand fluorines shows a characteristic splitting of 4.42 G more or less independent of the direction of the magnetic field. Its resolution, however, varies. Only with H along the $\langle 111\rangle$ direction can the typical intensity distribution[22] of the fluorine structure 1:8:28:56:70:56:28:8:1 be observed. It arises from the interaction with 8 equivalent fluorine nuclei of $I=\frac{1}{2}$ and is the final proof of the model of an isolated d ion in cubic symmetry.

The linewidth and the amplitude of the hyperfine pattern depend markedly on the nuclear quantum number. Since they are also temperature-dependent it is suggested that the broadening is due to spin-lattice relaxation. Using data taken at both 9 and 24 GHz, it is found that the linewidth depends on $|\Delta g\beta H_0+KM|$. Such a behavior has been predicted by McConnell[23] for a quite different case, namely spin-lattice relaxation of microcrystals in a liquid. A spin coupled to a nucleus is allowed to lose its orientation in a characteristic time τ_c. The resulting relaxation time becomes in this case

$$T_1^{-1}\sim\frac{(2/15\hbar^2)(\Delta g\beta H_0+KM)^2\tau_c}{(1+4\pi\nu_0^2\tau_c^2)},\qquad(36)$$

where ν_0 is the EPR frequency. The relaxation mechanism in our case has some resemblance to that of

TABLE IV. Linewidth of EPR transitions between tunneling states. The transition occurring at the lowest magnetic field is arbitrarily labeled $M=-\frac{7}{2}$.

State	Temperature	Linewidth in gauss for transition with $M=$ $-\frac{7}{2}$	$-\frac{5}{2}$	$-\frac{3}{2}$	$-\frac{1}{2}$	$\frac{1}{2}$	$\frac{3}{2}$	$\frac{5}{2}$	$\frac{7}{2}$
Γ_8, $H \parallel \langle 111\rangle$	1.5	2.7	2.8	2.9	3.0	3.2	3.3	3.7	4.2
	4.2	4.0	3.7	3.7	4.0	4.2	4.4	5.2	6.0
Γ_6	6	8.4	7.6	6.6	7.4	8.0	8.4	9.0	9.6
	14	8.3	7.7	7.2	7.7	8.1	9.5	10.	11.
Γ_7	54	All 12.5							
	77	All 26							

[22] J. E. Drumheller, J. Chem. Phys. **38**, 970 (1963).
[23] H. M. McConnell, J. Chem. Phys. **25**, 709 (1956).

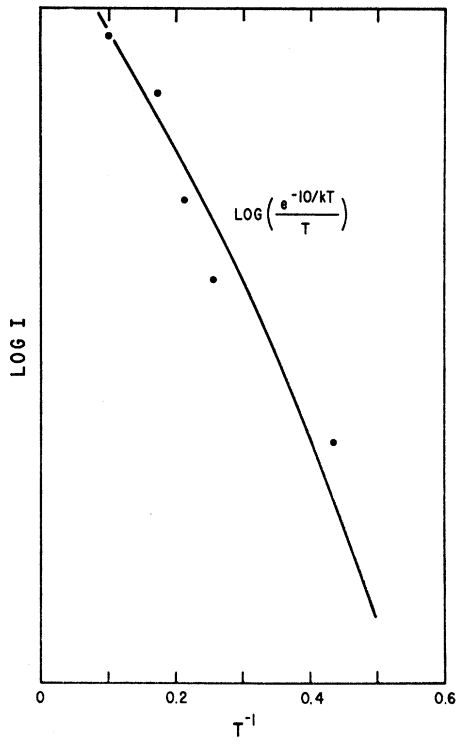

FIG. 13. Intensity of Γ_6 transitions as a function of temperature.

McConnell's model in that a transition ω_{68} or ω_{88} (Fig. 3) involves some reorientation of the Jahn-Teller complex with respect to the lattice. Using this model as a guide we can account for a few observations.

If the magnetic field is parallel to a ⟨111⟩ axis, only transitions between Γ_6 and Γ_8 contribute to the relaxation, $\omega_{88}=0$. Correspondingly, the lines are rather narrow and the superhyperfine structure is well resolved. Using theoretically calculated multicomponent spectra[24], the linewidths were evaluated. They are given in Table IV. If the magnetic field is in any other direction than ⟨111⟩, then ω_{88} contributes noticeably to the linewidth. Since the superhyperfine structure is irregular, even for $H\|\langle 100\rangle$, it was impossible to evaluate the linewidths in this case. It is, however, evident by inspection that the lines are narrowest, where $|\Delta g\beta H_0+KM|\sim 0$. This is the case for $M=-\frac{3}{2}$ at 9 GHz (Fig. 4) and for $M=-\frac{7}{2}$ at 24 GHz (Fig. 11). It may, however, turn out that a quantitative description of the relaxation time in terms of (36) is impossible, since (36) has been calculated for the classical limit of no tunneling.

An attempt has been made to determine the linear Jahn-Teller coefficient by measuring the change of population and the g shift as a function of uniaxially applied stress. With the stress applied in the ⟨100⟩ direction and the natural cleavage planes of the sample perpendicular to ⟨111⟩, the breaking limit of the sample was only 250 kg/cm². Up to this limit no effect on the paramagnetic spectrum was detected.

At temperatures above ~6°K, an isotropic spectrum is observed (Fig. 12). Its intensity increases with temperature as given in Fig. 13. It can be fitted to

$$I\sim T^{-1}\exp(-3\Gamma/kT), \tag{37}$$

indicating an excited state. We identify it as the symmetric state Γ_6. The excitation energies are

$$3\Gamma=10\ \text{cm}^{-1}\quad\text{for}\quad CaF_2\text{:Sc}$$

$$3\Gamma=8\ \text{cm}^{-1}\quad\text{for}\quad SrF_2\text{:Sc}.$$

3Γ is called the tunnel splitting.

The g factor and hyperfine constant of the Γ_6 state are given in Table II. As predicted by theory they constitute an average of the corresponding pairs of parameters evaluated from data taken at 6°K with the magnetic field parallel to ⟨100⟩. The linewidths depend on the nuclear quantum number indicating some relaxation to the Γ_8 state. A set of linewidths is given in Table IV.

Between 6 and 10°K they are practically independent of temperature. This suggests that this spectrum be attributed to the symmetric state rather than a motional average of the Γ_8 state. Especially the fact that at 4.2 and 5°K, transitions of both states can be seen simultaneously supports this statement. At higher temperature the lines broaden and they become less and less dependent on the nuclear quantum number.

If it is assumed that each transition has the same intensity, one can conclude that part of the apparent linewidth is due to poorly resolved superhyperfine structure. The best fit is reached for $A_F\sim 2$ G.

Above 45°K the hyperfine lines have the same width and intensity. This is shown in Fig. 14. A strong line at $g=2$ is superimposed to the Sc spectrum. Two pairs of weak lines outside of the octet should be disregarded as well. The linewidth can be expressed as a function

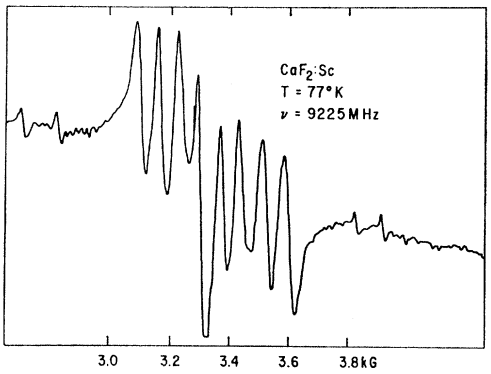

FIG. 14. EPR spectrum of CaF_2:Sc at 77°K. The rotational state. Besides the Sc spectrum a strong line at $g=2$ and four weak lines are seen. They are not analyzed.

[24] Ya. S. Lebedev, N. N. Tikhomivova, and V. V. Voevodskii, *Atlas of Electron Spin Resonance Spectra* (Consultants Bureau, New York, 1964), Vol. 2.

of temperature

$$\Delta H=\Delta H_0+\Delta H' \exp(-\Delta/kT), \qquad (38)$$

with $\Delta\sim 250$ cm^{-1} for CaF_2:Sc. The corresponding value for SrF_2:Sc is uncertain, it seems slightly lower. Unlike as in similar cases[25] the temperature-dependent part of (38) should be attributed to a relaxation process involving optical phonons. According to neutron scattering data by Cribier *et al.*[26] there should be a transverse optical mode at 7.75×10^{12} Hz corresponding to about 250 cm^{-1}. The lack of any dependence of the relaxation time on nuclear quantum number suggests this spectrum is due to the rotational Γ_7 state. Since the g factors are the same as for the Γ_6 state (both theoretically and experimentally), it is not possible to determine its excitation energy.

V. CONCLUSIONS

We try here to establish some relevant parameters of the Jahn-Teller potential. It has, however, to be borne in mind that we have made some approximations in order to simplify the theory. By confining the nuclear motion to β space we have assumed that $\hbar$ times the radial frequency ω is large compared to the tangential part of the nuclear kinetic energy $\hbar^2/2M\rho_0^2$. This allowed us to express our vibronic wave functions as sums of Born-Oppenheimer products involving zero point vibrations only. From the following evaluation of ω and ω' it will become evident that this approximation is not too well justified.

Using the harmonic approximation one finds

$$\gamma\sim\exp(-3V_0/2h\omega') \qquad (39)$$

and can estimate $V_0\sim h\omega'$. This says that only zero point vibration with an energy of about $\frac{1}{2}(h\omega')$ can be considered localized. The presence of only one localized vibronic state is reflected in the experimental data: The overlap does not increase with temperature (Fig. 9), excluding the possibility that excited localized states with greater overlap be populated.

The tunnel splitting, as estimated in the last section, is given by Eq. (29). Using the estimate above and the experimental value for $3\Gamma=10$ cm^{-1}, one finds

$$h\omega'\sim 50 \text{ cm}^{-1}, \qquad V_0\sim 50 \text{ cm}^{-1}.$$

If we use the frequency of the ϵ_g mode[26]

$$\omega\sim 250 \text{ cm}^{-1},$$

we can estimate the Jahn-Teller energy by means of (30):

$$E_{JT}\sim 2500 \text{ cm}^{-1}.$$

These values seem very reasonable and tend to indicate that it is possible to map the Jahn-Teller potential using EPR data. A determination of the tunnel potential V_0 by accoustic loss measurements would check the accuracy of the present method and thereby determine the validity of the theory.

We have shown that quantum mechanical tunneling can link equivalent vibronic states of a Jahn-Teller complex together. The resulting states are described by symmetrized wave functions and split by the tunnel splitting. The paramagnetic properties are those of Γ_6, Γ_7, and Γ_8 states of cubic symmetry, however the g anisotropy is reduced by almost 50%. A similar effect has been predicted by Ham[14,19] for a Γ_5 triplet orbital state, where the orbital-angular momentum and trigonal fields are quenched by quantum-mechanical tunneling.

ACKNOWLEDGMENTS

I would like to express my gratitude to Dr. M. D. Sturge for helpful correspondence and discussions. A suggestion by Professor C. Y. Huang is acknowledged as well. I am further indebted to a number of colleagues, particularly Dr. W. C. Holton for encouragement and help with the manuscript. My special gratitude is due to Dr. F. S. Ham who helped my understanding a number of times and pointed out the relation between strain and tunnel splitting to me.

[25] U. T. Höchli, K. A. Müller, and P. Wysling, Phys. Letters **15**, 5 (1965).
[26] D. Cribier, B. Farnoux, and B. Jacrot, Phys. Letters **1**, 187 (1962).